TU Delft

Delft University of Technology

Document Version
Final published version

Licence
CC BY

Citation (APA)
Chaparro López, M. J., Molina-Gómez, F., Castillo-Betancourt, J. P., Cabrera, M. A., Naranjo, J., Viana da Fonseca, A., & Caicedo, B. (2026). Dynamic mechanical analysis for sands using a shear rheometer: Experimental procedure and benchmarking with conventional tests. *Soil Dynamics and Earthquake Engineering*, *210*, Article 110509. https://doi.org/10.1016/j.soildyn.2026.110509

Important note
To cite this publication, please use the final published version (if applicable).
Please check the document version above.

Copyright
In case the licence states “Dutch Copyright Act (Article 25fa)”, this publication was made available Green Open Access via the TU Delft Institutional Repository pursuant to Dutch Copyright Act (Article 25fa, the Taverne amendment). This provision does not affect copyright ownership.
Unless copyright is transferred by contract or statute, it remains with the copyright holder.

Sharing and reuse
Other than for strictly personal use, it is not permitted to download, forward or distribute the text or part of it, without the consent of the author(s) and/or copyright holder(s), unless the work is under an open content license such as Creative Commons.

Takedown policy
Please contact us and provide details if you believe this document breaches copyrights.
We will remove access to the work immediately and investigate your claim.

This work is downloaded from Delft University of Technology.

Soil Dynamics and Earthquake Engineering 210 (2026) 110509

Contents lists available at ScienceDirect

Soil Dynamics and Earthquake Engineering

journal homepage: www.elsevier.com/locate/soildyn

Dynamic mechanical analysis for sands using a shear rheometer: Experimental procedure and benchmarking with conventional tests

María Juliana Chaparro López [a,*], Fausto Molina-Gómez [b], Juan-Pablo Castillo-Betancourt [a], Miguel Angel Cabrera [c], José Naranjo [a], António Viana da Fonseca [d], Bernardo Caicedo [a]

[a] Department of Civil and Environmental Engineering, Universidad de los Andes, Carrera 1E #19A-40, Mario Laserna (ML) Building, Piso 6, Bogotá, 111711, Colombia
[b] Department of Structures and Building Physics, Universidad Politécnica de Madrid, Av. Juan de Herrera 4, Madrid, 28040, Spain
[c] Faculty of Civil Engineering and Geosciences, Delft University of Technology, Stevinweg 1, Delft, CN, 2628, the Netherlands
[d] CONSTRUCT-GEO, Universidade do Porto (FEUP), Rua Dr. Roberto Frias, s/n, Porto, 4200-465, Portugal

ARTICLE INFO

Keywords:
Dynamic shear modulus
Low confining pressure
DMA rheometer
Small-strain stiffness
Cyclic loading
Element testing

ABSTRACT

Dynamic mechanical properties such as shear modulus (G) and damping ratio (ξ) are key parameters governing soil response under cyclic loading. However, evaluating these properties in loose dry sands under low confining pressures over a wide strain range ($\gamma = 10^{-6}$–10^{-2}) remains challenging using a single testing method. Dynamic Mechanical Analysis (DMA) addresses this limitation by enabling measurements across both small- and large-strain ranges within a single test. Although DMA is widely used in asphalt engineering, its application to geotechnical materials is relatively recent. Previous studies have adapted shear rheometers to perform DMA on loose sands. Nevertheless, the benchmarking with traditional methods remains limited.

This study presents a detailed DMA procedure for loose sands and benchmarks its results against conventional dynamic testing methods, including Resonant Column (RC) and Bender Element (BE) tests. The material tested is TP-Lisbon sand, a natural alluvial sand with subangular particles; it was tested under different confining pressures σ_3 = [10-50]kPa. The results demonstrate that DMA successfully captures shear modulus degradation and damping ratio evolution over the investigated strain range, showing good agreement with conventional laboratory techniques and confirming the method's reliability for dynamic soil characterization.

1. Introduction

Cyclic loads on soil propagate through the soil grain contact network. This propagation may shift and rearrange the contact network under high strain, allowing some grains to move freely and leading to irreversible strains [1–3]. The strain-dependent soil response is controlled by characteristics such as grain size, density, and confining pressure, among others [1,4,5]. This behavior is mainly described through two key properties, the shear modulus (G) and the damping ratio (ξ) [1,2,6,7].

At low confining pressures, the mechanical response of granular soils becomes increasingly governed by interparticle contact mechanics. The reduction in normal contact forces decreases contact stiffness and amplifies the influence of particle-scale characteristics such as grain shape, surface roughness, and contact rearrangement [1,8–10]. Consequently, small variations in stress state and shear strain application may produce significant changes in stiffness degradation and energy dissipation, making the characterization of dynamic properties particularly challenging for loose sands under low confinement [1,3,8]. As shear strain increases, contact rearrangement and particle sliding become more pronounced, leading to progressive degradation of the contact network and a reduction in soil stiffness [1,11].

Conventional methods measure the dynamic properties within specific strain ranges. For instance, in situ seismic methods capture the elastic domain at very small shear strains, $\gamma = [10^{-6}$–$10^{-5}]$ [1], while laboratory devices extend the coverage to broader ranges [2,11,12]. Resonant column testing characterizes low strains up to the elasto-plastic transition, $\gamma = [10^{-5}$–$10^{-3}]$ [2,13,14]. In contrast, cyclic triaxial devices operate at higher strains in the plastic range ($\gamma = [10^{-3}$–$10^{-2}]$) and require local instrumentation to improve

* Corresponding author.
E-mail addresses: mj.chaparro@uniandes.edu.co (M.J. Chaparro López), fausto.molina@upm.es (F. Molina-Gómez), jp.castillo11@uniandes.edu.co (J.-P. Castillo-Betancourt), m.a.cabrera@tudelft.nl (M.A. Cabrera), jnaranjo@uniandes.edu.co (J. Naranjo), viana@fe.up.pt (A. Viana da Fonseca), bcaicedo@uniandes.edu.co (B. Caicedo).

https://doi.org/10.1016/j.soildyn.2026.110509
Received 20 February 2026; Received in revised form 10 June 2026; Accepted 25 June 2026
Available online 8 July 2026
0267-7261/© 2026 The Authors. Published by Elsevier Ltd. This is an open access article under the CC BY license (http://creativecommons.org/licenses/by/4.0/).

resolution [12]. Therefore, a full assessment of G and ξ across strains of $\gamma = [10^{-6}–10^{-2}]$ demands combining multiple devices [15]. However, this integration may yield discontinuities, particularly under very low confining pressures [16]. Under these conditions, the dynamic response becomes highly sensitive to the stress state and the characteristics of the contact network, complicating the comparison and integration of measurements from different testing techniques [1,6,10]. Hence, a single device capable of spanning the entire strain range would improve the efficiency of measuring dynamic soil properties [17].

Dynamic Shear Rheometers used for Dynamic Mechanical Analysis (DMA) enable the evaluation of a wide shear strain range, $\gamma = [10^{-6}–10^{-2}]$, by applying harmonic torsional loading at controlled frequency and amplitude. The DMA is a technique originally developed to characterize the viscoelastic response of materials subjected to cyclic loading [7,14]. The method applies harmonic loading at controlled frequency and amplitude while continuously measuring the resulting stress-strain response. These measurements are used to determine the shear modulus (G) and damping ratio (ξ) over a broad strain range [18,19]. DMA has been extensively employed in polymer, asphalt, food, and biomaterial engineering to evaluate stiffness and damping properties over broad deformation ranges [7,18,19]. In geotechnical engineering, Villacreses et al. (2020) [14] adapted this methodology to characterize the dynamic response of partially saturated fine-grained soils. However, extending DMA to granular cohesionless soils requires the use of confinement systems to maintain specimen stability during testing [6]. Recent studies by Chaparro-López et al. (2023) [6] and Caicedo et al. (2025) [1] adapted this approach for loose sands, demonstrating the feasibility of measuring G and ξ under low confining pressures.

Compared with conventional dynamic testing methods, the proposed DMA approach enables characterization of both shear modulus degradation and damping ratio evolution over a wide strain range ($\gamma = 10^{-6}–10^{-2}$) using a single specimen and a single testing procedure. This reduces the need to combine results from multiple laboratory techniques and provides a unified framework for dynamic soil characterization under low confining pressures. Although previous studies have demonstrated the potential of DMA to evaluate the dynamic properties of loose sands under low confining pressures. The comparison with conventional geotechnical testing methods remains limited. Furthermore, detailed guidance on specimen preparation and confinement implementation remains limited, hindering other laboratories' adoption of the technique.

Consequently, the main objective of this research is to benchmark DMA results against conventional approaches, specifically the bender element and resonant column methods. In addition, it provides a detailed description of the methodology for laboratories seeking to replicate the procedure. For this purpose, TP-Lisbon sand is tested, and its DMA results are compared with resonant column data reported by Molina-Gómez et al. (2020) [13] and with bender element results reported by Molina-Gómez and Viana da Fonseca (2021) for the same material [20].

2. Methodology

2.1. Methods

A modified Dynamic Shear Rheometer (DSR) by TA Instruments AR2000 rheometer [21] performs the DMA tests. The system consists of a fixed bottom pedestal and a rotating top plate that applies cyclic torque to the specimen. This configuration subjects the sample to torsional shear under well-controlled conditions (see Fig. 1a). The DSR tests apply torsional loads similar to those used in the Cyclic Torsion Test configuration. However, the Cyclic Torsional commonly applies a shear strain range of $\gamma = [10^{-4}\text{-}10^{-3}]$ [2,15].

The DSR used in this research has a minimum torque oscillation of 3×10^{-8} N m and a minimum steady torque of 5×10^{-8} N m. The DSR can apply a maximum torque of 0.2 N m, with a resolution of 1×10^{-9} N. Additionally, the motor has an inertia of 15 μN m and can apply an angular velocity in the range of 1×10^{-8} rad/s to 300 rad/s, with a displacement resolution of 4×10^{-8} rad. The device directly measures shear stress and shear strain as a function of time, enabling the evaluation of shear modulus (G) and damping ratio (ξ) across a wide strain range [6,15,21].

The DMA tests were performed using a strain-sweep methodology, in which a sinusoidal torsional strain signal with a 1-min period was applied. At the same time, the corresponding shear stress was recorded. The tests were conducted under strain-controlled conditions. Each

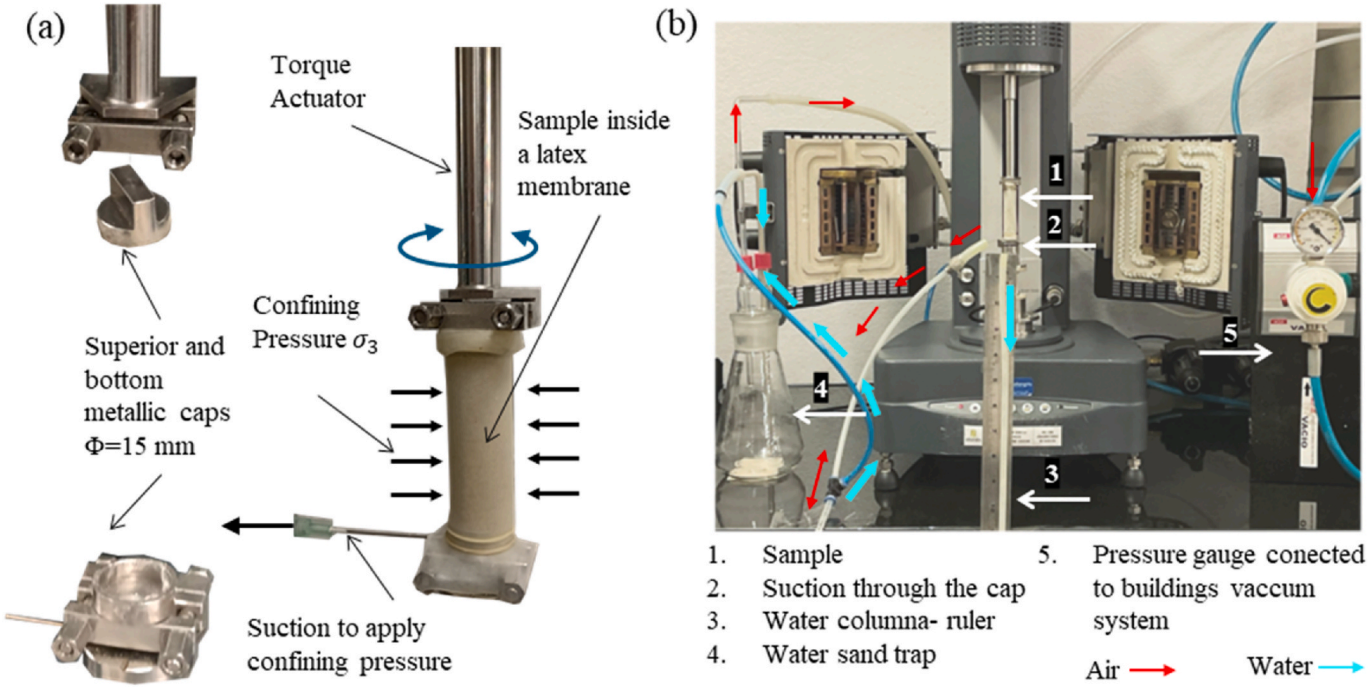

Fig. 1. Modified DMA setup. (a) System components (b) Water column method designed for better precision for $\sigma_3 \leq 10$ kPa.

strain-sweep consisted of 14 incremental shear strain levels within the range $\gamma = [10^{-6} - 10^{-2}]$. At each level, the specimen was subjected to 10 harmonic oscillations with a period of 1 min. Each oscillation generated one hysteresis loop, which was recorded to evaluate the evolution of the shear modulus (G) and damping ratio (ξ) with increasing strain amplitude. This procedure was adapted from the DMA tests on kaolin samples performed by Villacreses et al. (2020) [15].

Adapting the DSR for granular materials required specific modifications, since cohesionless soils cannot remain stable without lateral support. In previous research by Chaparro-López et al. (2023) [6] and Caicedo et al. (2024) [1], the DMA setup was modified to apply basal suction (σ_v), generating a confining pressure (σ_3) suitable for testing dry sand specimens. In this configuration, the specimen is encapsulated in a latex membrane and positioned between two aluminum caps, providing lateral support during torsional loading. The confinement system (Fig. 1a) consists of aluminum caps (15 mm in diameter), a latex membrane (15 mm in diameter, 60 mm in height, and 0.8 mm in thickness), a PVC support pipe (15 mm in diameter, 45 mm in height, and 3 mm in thickness), and two rubber O-rings (15 mm in diameter and 1 mm in thickness). The detailed procedure for membrane fabrication is presented in Appendix A. The basal suction is applied through the bottom cap using a 1000 mbar vacuum pump (AGA VALVULA EVAC 1000) connected to a vacuum airline [6]. For $\sigma_3 \leq 10$ kPa, a water column can be added in parallel with the suction line to improve the precision of the pressure readout. In this case, a water trap creates a vertical column whose level provides a visual and accurate indication of the applied suction, without contacting the specimen or the airline (Fig. 1b).

Specimens are built on a PVC mold, resulting in samples with a diameter of 15 mm and a height of 45 mm. Sand is deposited through a funnel to achieve a target relative density of $D_r = 0.30 \pm 0.05$. The latex membrane is first seated on the bottom cap and supported by the PVC mold. Sand is then poured while the upper plate remains raised. Once the target height is reached, the motor is lowered until the upper plate contacts the specimen. Finally, the membrane is vacuum-packed using O-rings at both caps. The membrane remains external to the device, allowing direct contact between the plates and the specimen (See Fig. 2).

The specimen dimensions (15 mm diameter and 45 mm height) were selected according to the requirements of the DMA testing configuration while maintaining a representative ratio between specimen size and particle size. As noted by Gourvès and Mezghani (1988), Gourvès (1993) [22,23] and Caicedo (2018) [24], a specimen diameter-to-particle size ratio greater than 10 ($d_{sample}/D_{max} > 10$) is required to obtain a coefficient of variation below 10% in the contact forces between particles. For the TP-Lisbon sand used in this study, the adopted specimen geometry satisfies this criterion by a wide margin, minimizing particle-size effects and supporting the assumption of continuum behavior [6,22–24].

2.2. Material

In this research, once the specimen preparation is completed, harmonic torsional loading is applied at a controlled frequency and amplitude. The device records shear stress and strain time histories that are later processed to compute G and ξ over the explored strain range.

The tested soil is TP-Lisbon, an alluvial natural soil collected near the Tagus River in Lisbon's city center. The mineral composition of TP-Lisbon sand consists of 78% quartz, 8% orthoclase, 8% muscovite, and 6% albite, as reported by Molina-Gómez et al. (2020) [14]. The predominance of quartz indicates that the material behaves as a cohesionless granular soil, in which interparticle contacts and frictional interactions primarily govern the mechanical response [1,14,25]. Fig. 3 shows its grain size distribution and physical properties. It also includes a scanning electron microscope (SEM) image, revealing that the grains in TP-Lisbon sand are primarily subangular [15].

2.3. Vertical stress and shear strain uniformity

Before testing the sand specimens, two checks are performed to ensure proper equipment performance. First, the vertical stress applied by the rheometer top cap must be checked to guarantee adequate friction between the cap and the sample. Second, the uniformity of the shear strain is confirmed to ensure that a homogeneous deformation is achieved across the specimen.

The axial stress (σ_1) is recorded for all confining pressures throughout the sweep strain tests (Fig. 4). The results show that σ_1 remains nearly constant over most of the strain range, with only minor fluctuations. A noticeable increase occurs at shear strains of

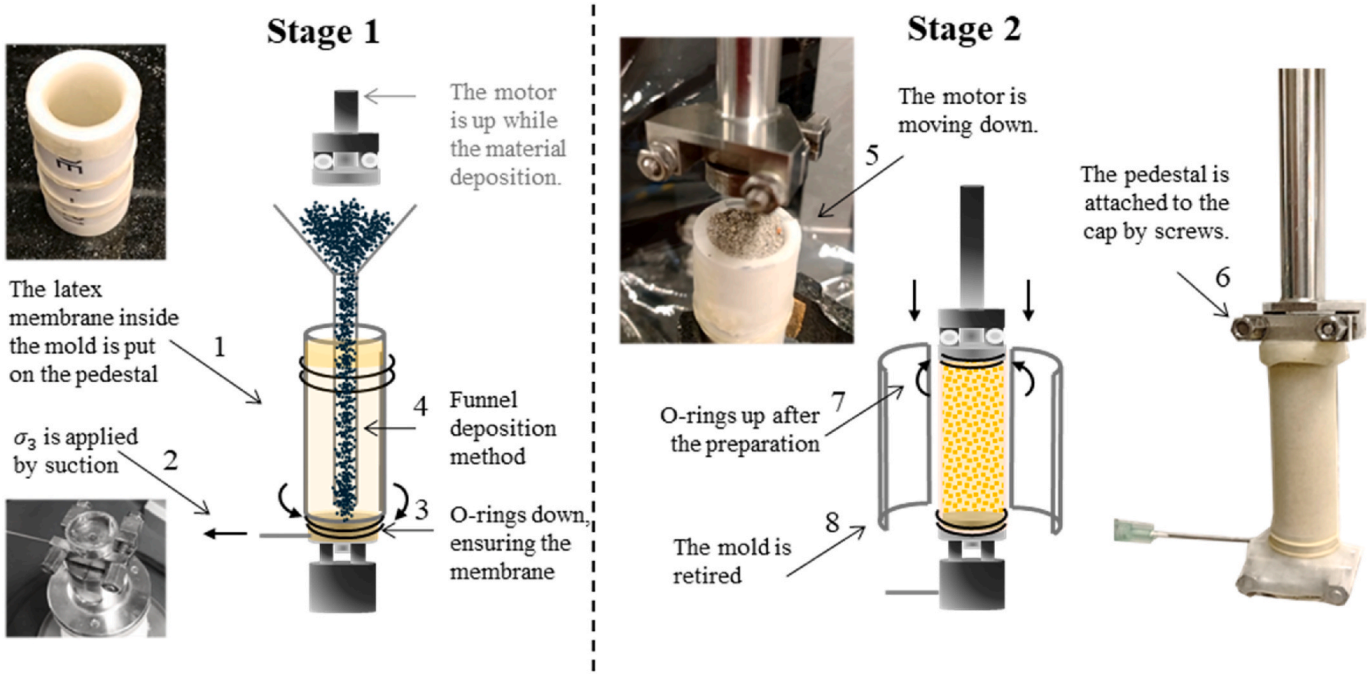

Fig. 2. Illustration of the sample preparation procedure.

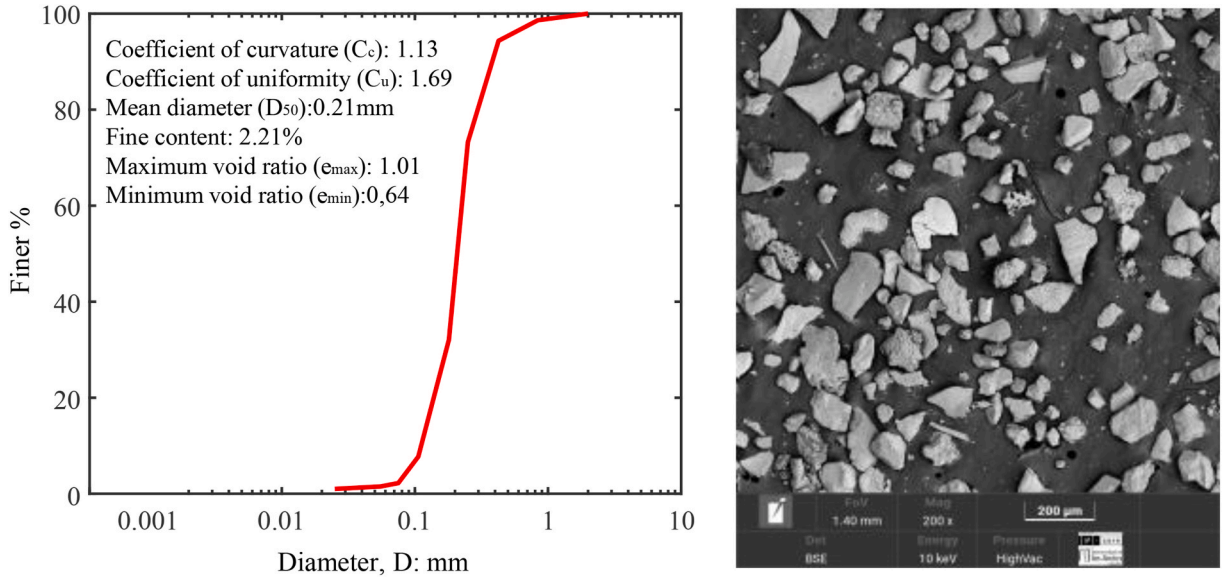

Fig. 3. Grain size distribution and SEM images of the TP-Lisbon sand.

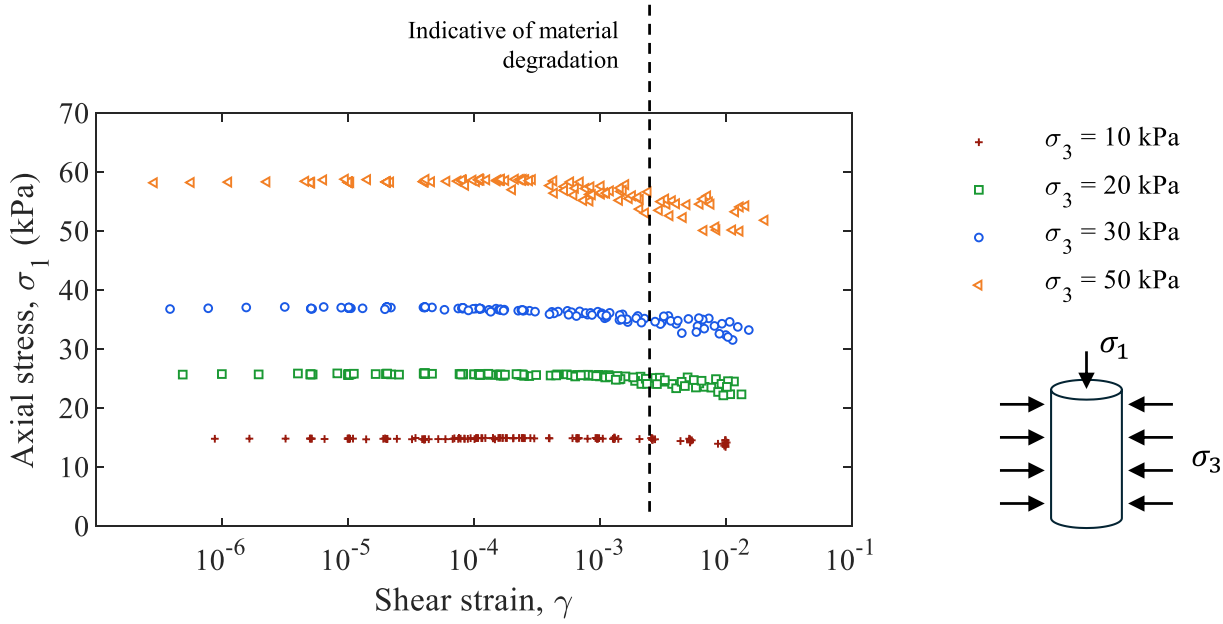

Fig. 4. Axial stress (σ_1) evolution during sweep strain tests for all confining pressures.

approximately ($\gamma > 10^{-3}$), coinciding with the onset of significant material degradation. Across tests, σ_1 is consistently 5 to 8 kPa above the applied confinement (σ_3), indicating a slightly anisotropic stress state ($\sigma_1 > \sigma_3$). The axial stress is induced because the contact between the rheometer upper cap and the specimen surface is required to ensure adequate torque transmission.

Image analysis confirms that shear deformation develops uniformly along the specimen height. Circumferential displacements are tracked using four visual markers placed on the membrane at 5 mm intervals (Fig. 5a). The verification test is carried out on a specimen composed of TP-Lisbon sand mixed with approximately 35% glass beads with a diameter of 6 mm, which enhances the visibility of particle movement, under a confining pressure of $\sigma_3 = 5$ kPa. This specimen was used only for visual verification purposes, and no mechanical properties were obtained from these tests. Fig. 5a shows the displacement of a glass bead particle and the membrane at the largest strain level ($\gamma \approx 10^{-2}$).

To validate the image-based measurements against the rheometer records, two loading cycles at a shear strain of $\gamma \approx 10^{-2}$ are selected. The shear strain reported by the rheometer software is extracted for these cycles and compared with the strain calculated from image analysis using $\gamma = \Delta x/y$. The shear strains obtained from the image analysis ($\gamma = 0.0148$ and $\gamma = 0.0170$) show close agreement with those recorded by the device ($\gamma = 0.0142$ and $\gamma = 0.0165$), as illustrated in Fig. 5b. This agreement confirms that the deformation field remains uniform and that the cycles identified in the video correspond to those imposed by the rheometer. No visible membrane detachment, separation, or wrinkling was observed during testing. Significant membrane–soil slip would be expected to produce localized deformation or deviations from the observed displacement profiles. Since uniform deformation is verified at large strains, a similar consistency is expected at lower strain levels.

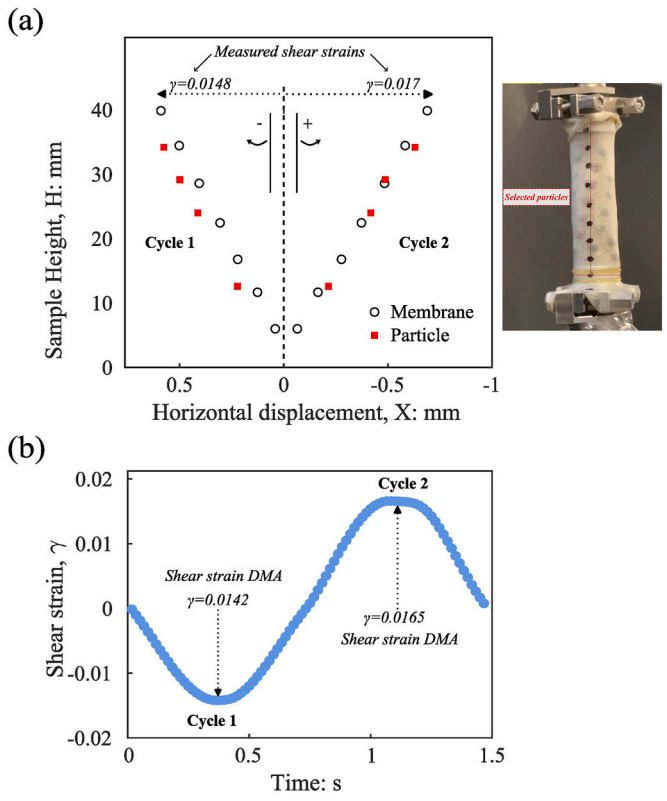

Fig. 5. Displacement profiles along the sample height for $\gamma = 10^{-3}$ and $\gamma = 10^{-2}$, confirming shear deformation under torsional loading.

2.4. Membrane effect

A calibration test was performed on the 0.8 mm latex membrane alone using the same testing configuration employed for the soil specimens. Fig. 6 compares the shear-modulus degradation and damping-ratio curves obtained for the membrane with those measured for a Fontainebleau sand specimen tested at a confining pressure of 10 kPa.

Fig. 6a shows that the membrane exhibits a shear modulus below 1 MPa throughout the investigated strain range, whereas the Fontainebleau sand specimen reaches a maximum shear modulus of approximately 30 MPa. Consequently, the membrane stiffness represents less than 3% of the measured specimen stiffness, indicating that its contribution to the overall shear modulus is negligible.

Fig. 6b presents the damping ratio obtained for both the membrane and the sand specimen. Although the membrane exhibits damping ratios of the same order of magnitude as those measured in the soil specimen, its stiffness remains substantially lower over the entire strain range. As a result, the amount of elastic energy stored and dissipated by the membrane is small compared with that of the soil specimen, and its influence on the measured damping ratio is expected to be limited.

3. Results and discussion

3.1. Dynamic mechanical analysis results

The mechanical response of the TP-Lisbon sand under cyclic shear loading is evaluated using Dynamic Mechanical Analysis (DMA). Strain-sweep tests are performed by varying the shear strain amplitude from $\gamma = 10^{-6}$ to 10^{-2} while maintaining a constant loading frequency of 1 Hz. This value was selected based on the frequency sweep study reported by Chaparro-López et al. (2023) [6], who evaluated Fontainebleau sand at $\sigma_3 = 5$ kPa over a frequency range of 0.01–1.8 Hz and observed relatively small variations in shear modulus and damping ratio. Therefore, a frequency of 1 Hz was adopted as a representative testing condition for the present study. At each strain level, ten loading cycles are applied. The sample is subjected to confining pressures of $\sigma_3 = 10$, 20, 30, and 50 kPa. Shear modulus and damping ratio are computed directly from the measured shear stress–shear strain time signals obtained during the strain-sweep procedure. The rheometer resolution allows stable stress–strain data to be captured even at very small strain levels ($\gamma \approx 10^{-6}$–10^{-5}), enabling direct estimation of hysteretic damping across the full strain range. Fig. 7a shows representative hysteresis loops obtained at $\sigma_3 = 30$ kPa as γ increases, computed from the recorded shear stress and shear strain signals (Fig. 7b).

Once the specimens are prepared and tested under the described confinement system, the strain-sweep results are analyzed. Fig. 8 presents the shear modulus degradation (G) curves and the evolution of the hysteretic damping ratio (ξ) with increasing confining pressure (σ_3). G increases with confinement due to enhanced contact forces, leading to a stiffer response.

The damping ratio (ξ) follows a consistent trend across pressures. However, greater dispersion is observed at higher shear strains ($\gamma > 10^{-3}$), consistent with the stiffness degradation observed in the modulus curves. At low confinement levels, particle contacts are more prone to rearrangement, leading to lower stiffness and further degradation. This behavior is evident at $\sigma_3 = 10$ kPa, where the elastic range is reduced, and damping deviates from the exponential trend observed at higher pressures.

The evaluation of dynamic behavior at low confinement is particularly relevant for shallow geotechnical systems such as surface foundations, road subgrades, and other structures subjected to dynamic loading [2,4,13]. In these conditions, limited confinement reduces stiffness and increases deformation, potentially affecting performance under cyclic loading. This testing configuration for the DMA test enables the shear rheometer to effectively characterize sands under low confining pressures, $\sigma_3 \leq 10$ kPa, typical of near-surface geotechnical conditions.

To benchmark the DMA methodology, comparisons are made with resonant column (RC) and bender element (BE) results reported for TP-Lisbon sand. RC provides the reference for the strain-dependent response, allowing direct comparison of the modulus degradation curve (G/G_{max}) and the damping ratio (ξ) trend over the strain range common to both devices. BE results are subsequently used to validate the small-strain shear modulus (G_{max}), offering an independent wave-based estimate. Together, these benchmarks assess the consistency of the DMA response from the elastic domain to the onset of nonlinear behavior under low confining stress.

3.1.1. Repeatability and correlation analysis

Fig. 9 shows three repetitions performed at each confining pressure. The repeatability of the DMA measurements was assessed by calculating the correlation coefficient for each confining pressure. The correlation coefficients obtained between repetitions ranged from 0.88 to 0.98, indicating a strong agreement in the shape of the shear modulus degradation curves. The highest correlations were observed at confining pressures of 30 and 50 kPa ($R > 0.98$), whereas slightly lower values were obtained at 20 kPa ($R \sim 0.88$). These results suggest that measurement repeatability improves as confinement increases and the contact network becomes more stable [26].

The variability between repetitions was also evaluated using the Coefficient of Variation (COV), calculated over the entire degradation curves. The average COV values ranged from 11.4% to 29.5%. Despite differences in the magnitude of the modulus, the overall shape of the degradation curves remained consistent across all repetitions [27].

3.2. Benchmark results with resonant column and bender elements

The normalized shear modulus degradation curves (G/G_{max}) and the evolution of the damping ratio (ξ) for confining pressures of $\sigma_3 = 30$ kPa and $\sigma_3 = 50$ kPa are compared with results obtained from existing

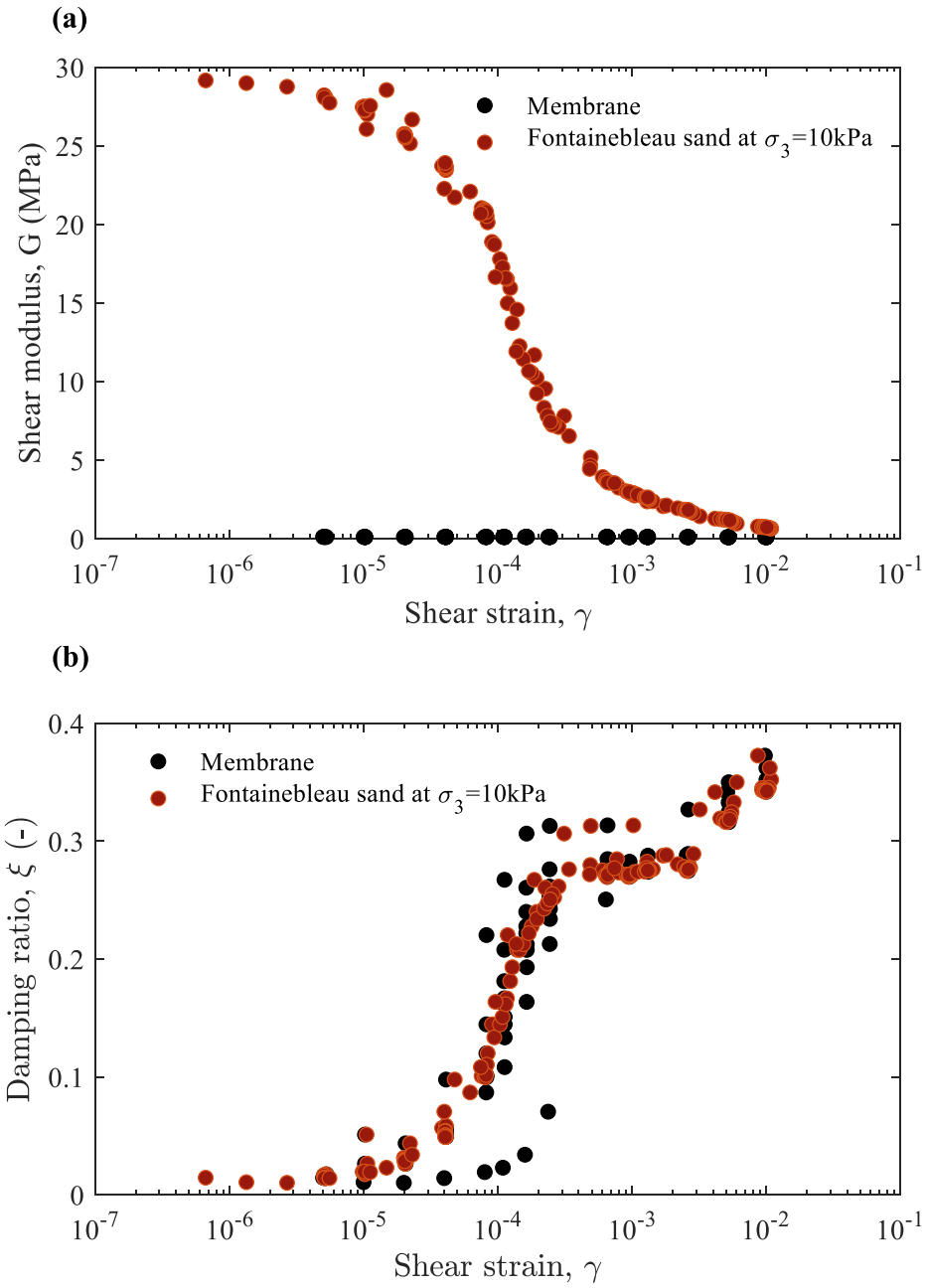

Fig. 6. Comparison between the dynamic properties of the latex membrane alone and a Fontainebleau sand specimen tested at σ_3 = 10 kPa: (a) shear modulus degradation and (b) damping ratio as a function of shear strain.

laboratory techniques, including the Resonant Column (RC) and Bender Element (BE) methods. The reference data is based on Molina-Gómez et al. (2020) [14]. In this research, the dynamic properties of TP-Lisbon sand, including the shear modulus degradation curve (G/G_{max}) and the damping curve (ξ), were tested using a resonant column device at a relative density of $D_r \approx 0.3 \pm 0.03$. Molina-Gómez et al. (2020) [14] also tested the maximum shear modulus of the TP-Lisbon sand using the Bender Elements (BE) device.

3.2.1. *Comparison of the shear modulus degradation curve G*

Fig. 10 compares the shear modulus degradation curves obtained from DMA and resonant column measurements together with the predictions of the Ishibashi and Zhang (1993) [11], Santos and Gomes (2001) [28], and Oztoprak and Bolton (2013) [29] models. All approaches exhibit the characteristic nonlinear reduction in normalized shear modulus with increasing shear strain, confirming that the DMA test captures the expected stiffness degradation behavior of loose sands.

Ishibashi and Zhang (1993) compiled available data on the dynamic shear moduli of various non-plastic sands and proposed a general equation relating shear modulus to confining pressure [11] (see Equations (1)–(3)). In this formulation, G/G_{max} represents the normalized shear modulus, defined as the ratio between the shear modulus at a given strain level and the maximum shear modulus (see Eq (1)). The parameter $K(\gamma)$ controls the shape of the degradation curve as the shear strain increases, while $m(\gamma)$ describes the effect of confining pressure on the shear modulus at a given strain level. The parameter m_0 corresponds to the value of m at zero shear strain [11]. In this model, σ_3 is the effective confining pressure (kPa), and γ is the shear strain amplitude. Where K and m are functions of the shear strain in the form of Equations (2) and (3).

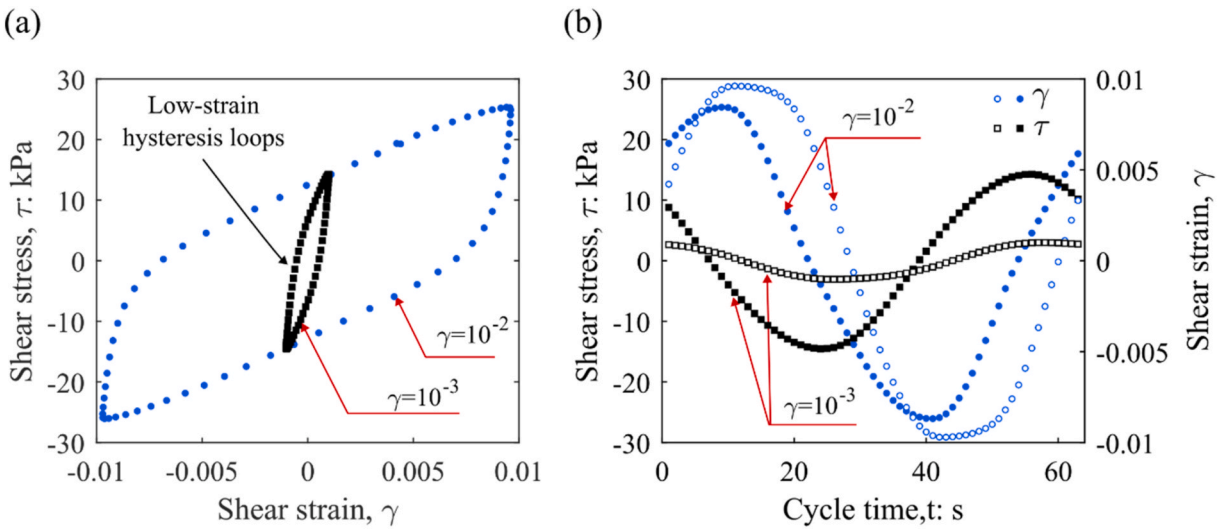

Fig. 7. (a) Hysteresis loops at a confining pressure of $\sigma_3 = 30$ kPa for two shear strain levels ($\gamma = 10^{-3}$ and $\gamma = 10^{-2}$), illustrating the nonlinear stress–strain response. (b) Time signal of shear stress τ and shear strain for $\gamma = 10^{-3}$ and $\gamma = 10^{-2}$.

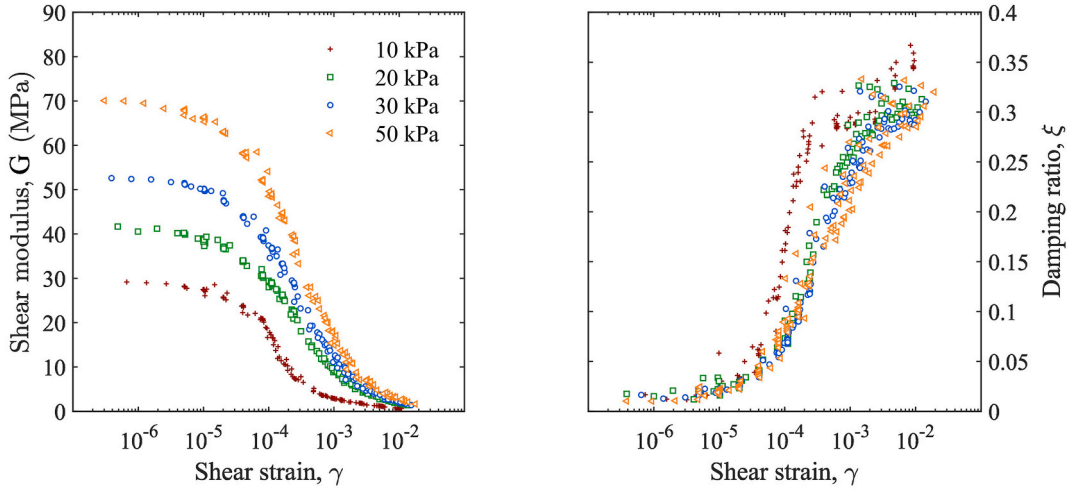

Fig. 8. Shear modulus (a) and hysteretic damping (b) for different confining pressures, σ_3 = [10, 20, 30, 50] kPa.

$$\frac{G}{G_{max}} = K(\gamma)\sigma_3^{-m(\gamma)-m_0} \quad \text{Eq 1}$$

$$K(\gamma) = 0.5\left[1 + \tanh\left\{\ln\left(\frac{0.000102}{\gamma}\right)^{0.492}\right\}\right] \quad \text{Eq 2}$$

$$m(\gamma) - m_0 = 0.272\left[1 - \tanh\left\{\ln\left(\frac{0.000556}{\gamma}\right)^{0.4}\right\}\right] \quad \text{Eq 3}$$

Santos and Gomes Correia [28], investigate the shear modulus degradation of soil with strain. The study was based on a key parameter previously defined by the authors, the reference threshold shear strain, $\gamma_{0.7}$. This parameter was defined as the shear strain for a normalized soil stiffness degradation factor of $G/G_{max} = 0.7$, in which G_{max} is the initial shear modulus for a very small strain ($\gamma = 10^{-6}$), and G is the secant modulus of soil. The authors proposed using a hyperbolic function to fit the test results. Simple regression analysis shows that the previous boundary curves can be fitted by a mean curve defined by the relationship shown in Eq (4). The best fit was obtained with a value of 0.385 using the least-squares method.

$$\frac{G}{G_{max}} = \frac{1}{1 + a\left(\frac{\gamma}{\gamma_{0.7}}\right)} \quad \text{Eq 4}$$

More recently, Oztropak and Bolton (2013) [29] calibrated the model's parameters to fit the results of 454 literature tests on granular soils. Additionally, the model parameters were determined through a detailed review of extensive experimental data collected on sands with various grain-size distributions [55]. Based on these calibrations, the model yields a relatively simple Eq (5).

$$\frac{G}{G_{max}} = \frac{1}{1 + \left(\frac{\gamma - \gamma_e}{\gamma_r}\right)^a} \quad \text{Eq 5}$$

where the normalized soil stiffness G/G_{max} can be estimated as a function of the shear strain γ, a reference shear strain γ_r an elastic threshold strain γ_e, and a curvature coefficient α, varying between 0.75 and 1.0 [29].

The comparison presented in Fig. 10 shows good agreement between the DMA measurements, RC results, and the predictive models. The agreement was quantified using the Mean Absolute Percentage Error

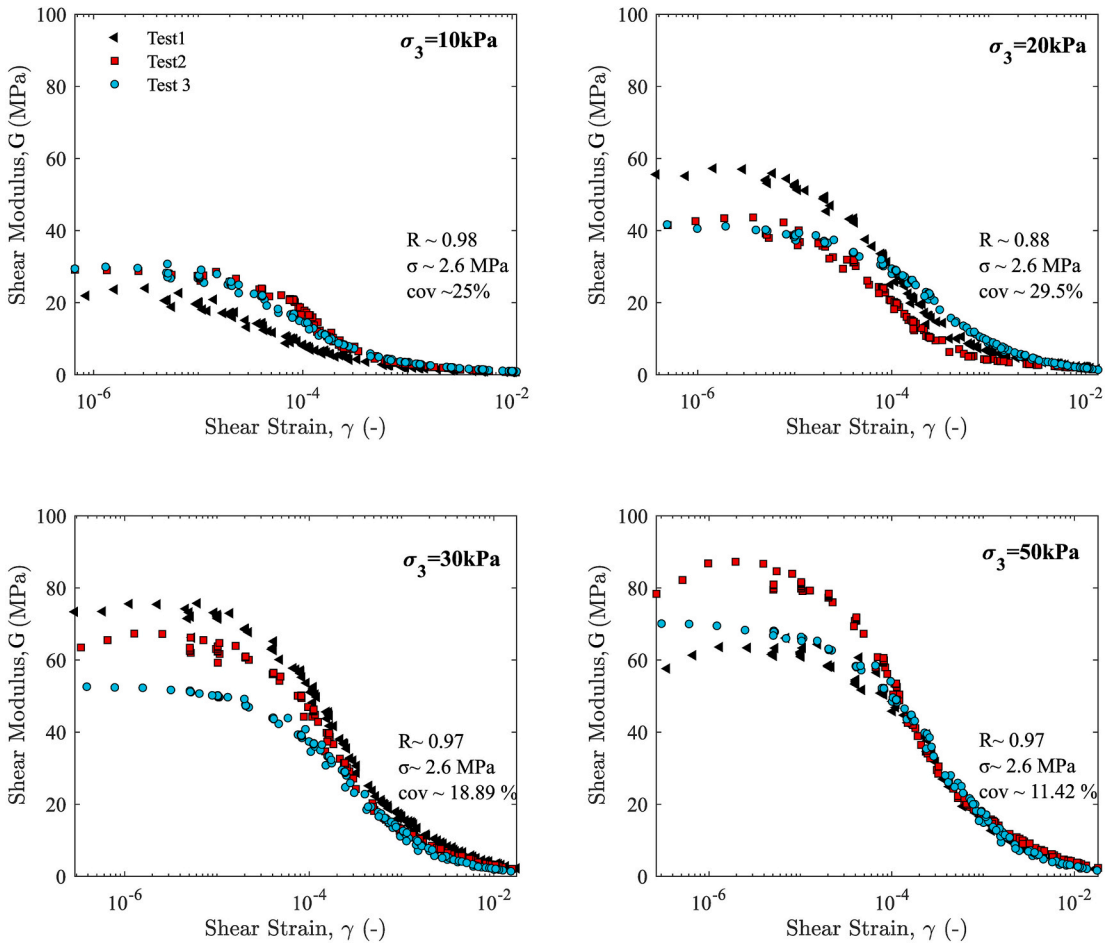

Fig. 9. Repeated tests for each confining pressure.

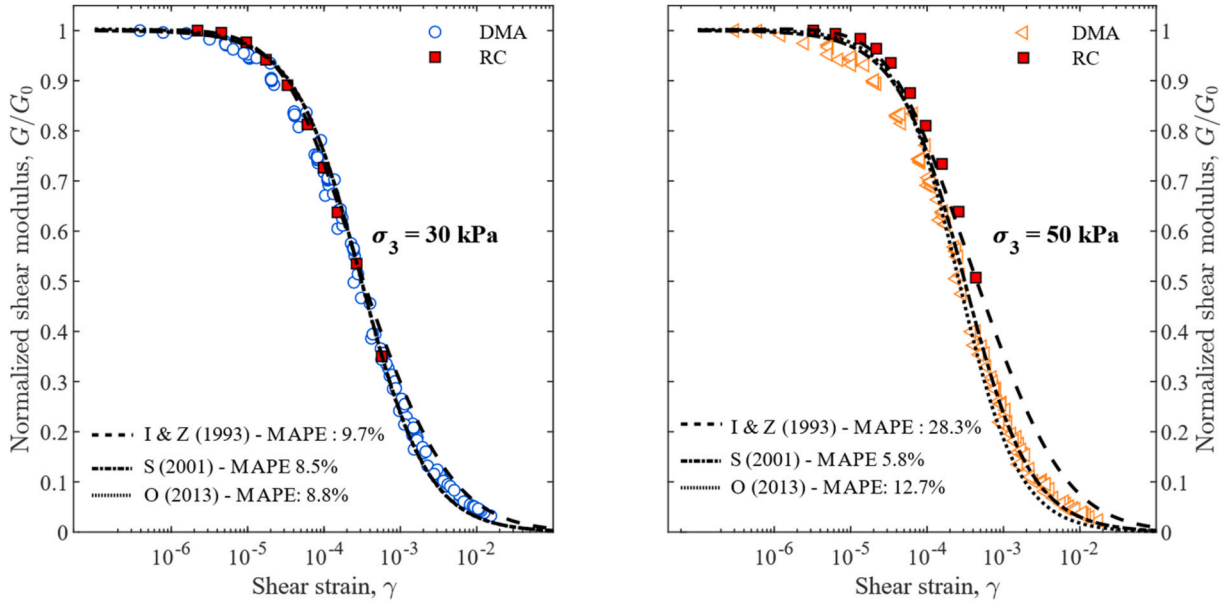

Fig. 10. Degradation curves of the Shear modulus between the DMA results and the resonant column (RC) by Molina-Gómez et al. [14], and their predictions by existing models: Ishibashi and Zhang (1993) (I&Z) [11], Santos and Gomes Correia (2001) (S) [28], and Oztoprak and Bolton (2013) (O) [29].

(MAPE) [30]. A MAPE value of 0% would indicate a perfect match between the compared datasets. At a confining pressure of $\sigma_3 = 30$ kPa, all comparisons yielded MAPE values below 10%, ranging from 4.1% for the RC measurements to 9.7% for the Ishibashi & Zhang model, indicating very good agreement. At $\sigma_3 = 50$ kPa, the Santos & Gomes Correia model provided the closest prediction to the DMA results, with a MAPE

of 5.8%, followed by Oztoprak & Bolton (12.7%) and the RC measurements (13.7%). In contrast, the Ishibashi and Zhang model exhibited a larger deviation (MAPE = 28.3%), particularly at intermediate and large strain levels. Overall, the results demonstrate that DMA provides measurements that are consistent with conventional laboratory testing and are well represented by existing shear modulus degradation models [30].

3.2.2. Comparison of damping ratio ξ

Comparing damping ratios is more challenging than comparing shear moduli because there are different methods for calculating energy dissipation in soils. The choice of method depends on the testing device and the material characteristics. In granular materials, for instance, damping is mainly associated with hysteretic effects in the stress–strain relationship, reflecting irreversible deformations [1,2]. In the DMA, sweep strain tests allow the determination of hysteretic damping from stress–strain loops (Fig. 11a), which could be related with the phase angle commonly used in viscoelastic materials (Fig. 11b). In contrast, in resonant column tests, damping is obtained from the solution of the dynamic equation governing the resonant response of the specimen (Fig. 11c) [14,17]. Although both methods quantify energy dissipation during cyclic loading, they are based on different physical principles. In the DMA, damping is directly associated with hysteretic energy losses occurring within the soil during each loading cycle. In contrast, the damping ratio obtained from RC tests reflects the attenuation of the resonant response of the specimen–device system and is commonly determined using the half-power bandwidth method. Nevertheless, the resulting damping values are very similar between the two methodologies.

Ishibashi and Zhang (1993) proposed an equation relating the damping ratio to G/G_{max}, which was fitted using Equation (4) [11].

$$\xi = 0.333\left\{0.586\left(\frac{G}{G_{max}}\right)^2 - 1.547\left(\frac{G}{G_{max}}\right) + 1\right\} \quad (4)$$

Fig. 12 compares the damping ratio ξ obtained from the Dynamic Mechanical Analysis (DMA) and resonant column tests with the predictions of the Ishibashi and Zhang model. The ξ results from the half-power method were lower, consistent with comparisons among methods for characterizing the damping evolution in granular soils [31–33]. The results have a MAPE range from 35% to 40%. This discrepancy can be attributed to the different measurement principles. The DMA quantifies hysteretic damping from stress-strain loops, and the damping ratio in the Resonant Column tests is derived from the solution of the dynamic equation governing the resonant-column system. Despite these methodological differences, both experimental approaches capture a consistent evolution of damping with increasing strain. Recent studies by Sun and Wang [17] also demonstrated that both techniques are comparable at low damping levels, which is consistent with the trends observed in Fig. 10.

3.2.3. Comparison of the maximum shear modulus with Bender Elements (BE)

For the small-strain range, the maximum shear modulus values obtained from the DMA tests are compared with those measured using bender element tests by Molina-Gómez and Viana da Fonseca (2021) for TP-Lisbon sand [14] (see Fig. 13). The BE specimens were prepared at a relative density of $D_r \approx 0.28 \pm 0.03$, whereas the DMA specimens were prepared at $D_r = 0.30 \pm 0.05$. Both methods exhibit a similar trend as confining pressure increases, with a MAPE of 18%. The observed differences may be associated with the slightly different relative densities of the specimens used in both studies, as well as the mildly anisotropic stress state induced by the rheometer configuration [34–38].

Despite the difference, the trend alignment supports the DMA's ability to accurately capture small-strain stiffness, a key parameter in seismic and vibration analyses. This consistency supports the validity of the DMA approach, especially given its ability to apply very low confining pressures and capture G_{max} within the same test used for higher strain levels, thereby eliminating the need for separate test setups.

Using DMA across the full strain range simplifies the testing procedure and avoids inconsistencies that can arise when combining multiple devices. This unified approach is particularly advantageous for characterizing surficial layers, where strain ranges and confinement vary widely. The comparison is also relevant because the reference measurements were obtained with different equipment and performed in different laboratories across two countries, thereby reinforcing the reliability of the rheometer results.

4. Concluding Remarks

This work presents the application of a modified Dynamic Mechanical Analysis (DMA) rheometer to characterize the dynamic shear modulus and damping ratio of TP-Lisbon sand. The method captures the complete transition from elastic to elasto-plastic behavior in a single test over the entire strain range ($\gamma = 10^{-6}$ to 10^{-2}), encompassing both small- and large-strain responses. This provides a new approach that eliminates the need to integrate test results from various testing procedures.

The results show a clear influence of confining pressure on shear modulus degradation, with higher confining pressure leading to greater stiffness and lower degradation. The damping ratio increases with strain, as expected from established models, demonstrating the DMA's capability to characterize both stiffness and energy dissipation within a single experimental framework across the entire deformation spectrum. This unified approach offers a practical and efficient alternative for evaluating the dynamic response of loose sands, particularly in shallow

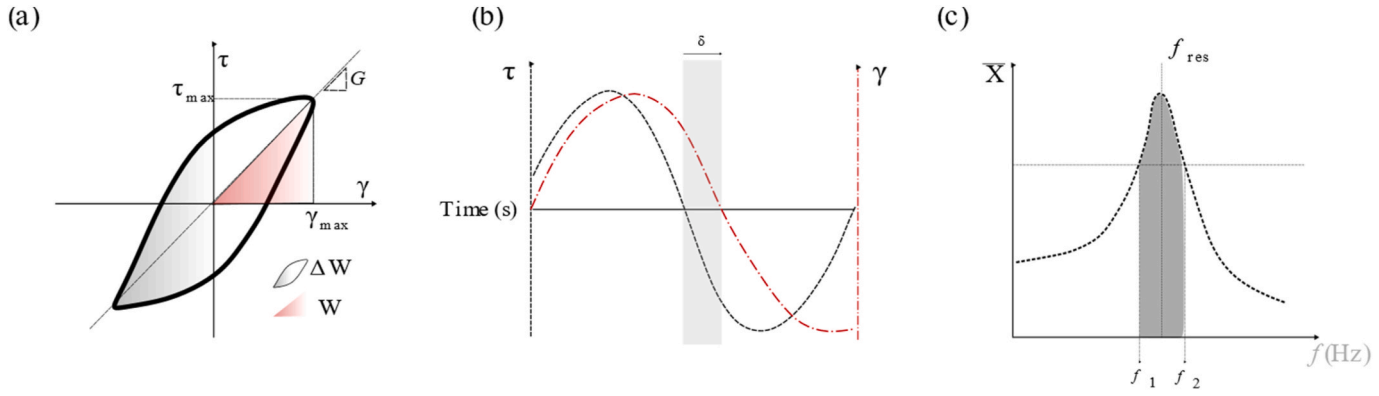

Fig. 11. Methods for estimating damping ratio: (a) hysteretic damping from DMA stress–strain loops, (b) energy dissipation represented by the phase angle, and (c) Method from RC tests [2,14,17].

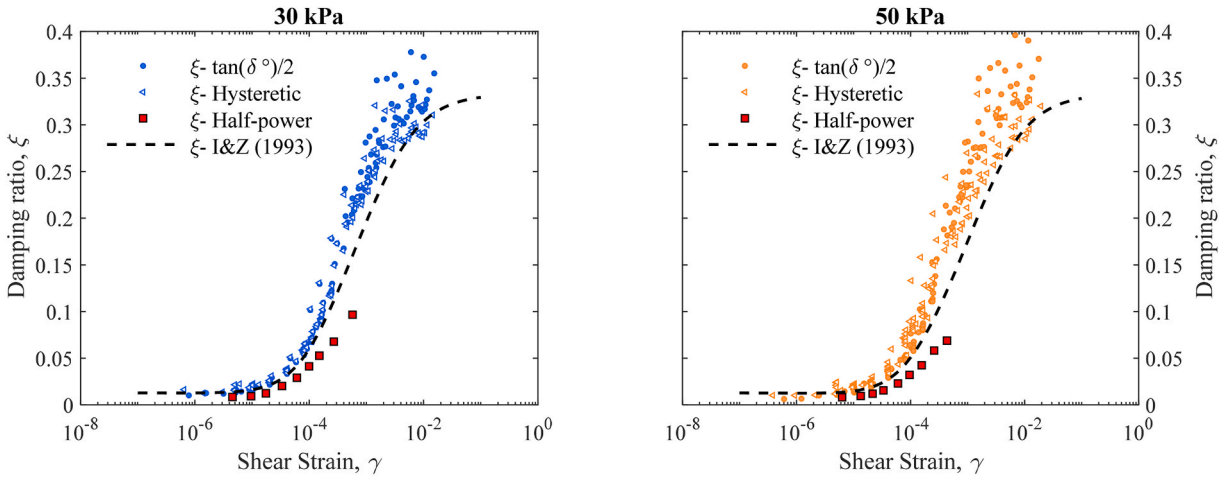

Fig. 12. Comparison of the different damping estimation methods, including DMA (phase angle and hysteretic loops), resonant column data from Molina-Gómez et al. [14], and the theoretical model by Ishibashi and Zhang (1993) [11]. The resultant Mean Absolute Percentage Error (MAPE) between the DMA results and the model for $\sigma_3 = 30$ kPa and $\sigma_3 = 50$ kPa is 35% and 36%, respectively.

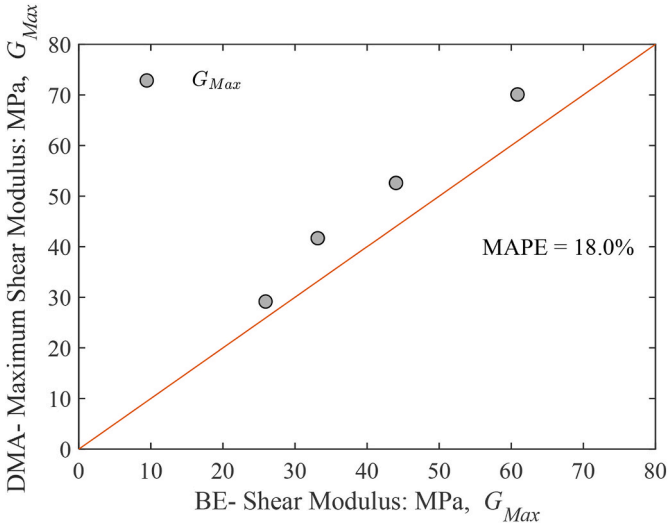

Fig. 13. Comparison of DMA tests and Bender Elements (BE).

geotechnical systems such as pavement subgrades, embankment foundations, and near-surface deposits subjected to traffic or seismic loading, where low confining pressures prevail, and traditional testing methods are often limited.

Comparisons of DMA results with resonant column and bender element tests on the same material and relative density reveal consistent trends in shear modulus under confining pressures of $\sigma_3 = 30$ kPa and $\sigma_3 = 50$ kPa. The damping ratio values obtained with the DMA also align well with those obtained from resonant column tests in the overlapping strain range. These confirm the reliability of the DMA for measuring small-strain stiffness, modulus degradation, and damping, reinforcing its applicability as a complementary or alternative method for dynamic soil characterization under low confining pressure conditions.

The procedure presented here is reproducible in standard DMA rheometers with minor adaptations and can be extended to other loose granular materials. However, the current configuration was developed for dry granular soils under low confining pressures. Extending the methodology to saturated soils would require additional modifications to the testing setup, including the use of a triaxial chamber to apply confining pressure and monitor pore-water pressures, allowing saturation to be verified through the Skempton B-value parameter. In addition, a fluid circulation system would be required to maintain hydraulic conditions during testing. Further research is therefore needed to assess the applicability of the proposed methodology to saturated soils and fine-grained materials.

Funding statement

This research did not receive any specific grant from funding agencies in the public, commercial, or not-for-profit sectors.

CRediT authorship contribution statement

María Juliana Chaparro López: Conceptualization, Data curation, Formal analysis, Investigation, Methodology, Visualization, Writing – original draft. **Fausto Molina-Gómez:** Conceptualization, Formal analysis, Validation, Writing – review & editing. **Juan-Pablo Castillo-Betancourt:** Data curation, Formal analysis, Investigation. **Miguel Angel Cabrera:** Conceptualization, Supervision, Validation, Writing – review & editing. **José Naranjo:** Data curation, Formal analysis, Investigation. **António Viana da Fonseca:** Supervision, Validation, Writing – review & editing. **Bernardo Caicedo:** Conceptualization, Funding acquisition, Project administration, Resources, Supervision, Validation, Writing – review & editing.

Declaration of competing interest

The authors declare that they have no known competing financial interests or personal relationships that could have appeared to influence the work reported in this paper.

Acknowledgements

The authors gratefully acknowledge the financial and laboratory support provided by Universidad de los Andes, Colombia.

Appendix B. Supplementary data

Supplementary data to this article can be found online at https://doi.org/10.1016/j.soildyn.2026.110509.

Data availability

Data will be made available on request.

References

[1] Caicedo B, Chaparro MJ, Castillo-Betancourt JP, Cabrera MA, Delage P, Lognonné P, Banerdt B. A micromechanical model for estimating the shear modulus and damping ratio of loose sands under low stress: application to a Mars regolith simulant. Geotechnique 2025;75(3):379–92. https://doi.org/10.1680/jgeot.23.00244.

[2] Ishihara K. Soil Behaviour in Earthquake Geotechnics. 1st ed. Oxford: Clarendon Press; 1996.

[3] Reddy NS, He H, Senetakis K. DEM analysis of small and small-to-medium strain shear modulus of sands. Comput Geotech 2022;141:104518. https://doi.org/10.1016/j.compgeo.2021.104518.

[4] Kramer SL. Geotechnical Earthquake Engineering. 1st ed. New Yersey: Pretince Hall; 1996.

[5] Poblete M, Wichtmann T, Niemunis A, Triantafyllidis T. Caracterizacion cíclica multidimensional de los suelos no cohesivos. Obras y Proyectos 2015;(17):31–7.

[6] Chaparro-López M-J, Castillo-Betancourt J-P, Cabrera M, Caicedo B, Delage P, Lognonné P, Banerdt B. Dynamic mechanical analysis test for evaluating loose sands on a wide strain range—application to the InSight mission on Mars. Geotech Test J 2023;46(6):901–20. https://doi.org/10.1520/GTJ20230381.

[7] Caro S, Sánchez DB, Caicedo B. Methodology to characterize non-standard asphalt materials using DMA testing: application to natural asphalt mixtures. Int J Pavement Eng 2015;16(1):1–10. https://doi.org/10.1080/10298436.2014.893328.

[8] Santamarina JC, Klein KA, Fam MA. Soils and waves: particulate materials behavior, characterization and process monitoring. Chichester: John Wiley & Sons; 2001.

[9] O'Sullivan C. Particulate discrete element modelling: a geomechanics perspective. Boca Raton: CRC Press; 2011. https://doi.org/10.1201/9781482266498.

[10] Cho G-C, Dodds J, Santamarina JC. Particle shape effects on packing density, stiffness, and strength: natural and crushed sands. J Geotech Geoenviron Eng 2006;132(5):591–602. https://doi.org/10.1061/(ASCE)1090-0241(2006)132:5(591).

[11] Ishibashi I, Zhang X. Unified dynamic shear moduli and damping ratios of sand and clay. Soils Found 1993;33(1):182–91. https://doi.org/10.3208/sandf1972.33.182.

[12] Rio JF. PhD diss. Advances in Laboratory Geophysics Using Bender Elements. London: University College of London; 2006.

[13] Irfan M, Cascante G, Basu D, Khan ZH. Novel evaluation of Bender element transmitter response in transparent soil. Geotechnique 2020;70(3):187–98. https://doi.org/10.1680/jgeot.17.P.256.

[14] Molina-Gómez F, Viana da Fonseca A, Ferreira C, Camacho-Tauta J. Dynamic properties of two historically liquefiable sands in the Lisbon area. Soil Dynam Earthq Eng 2020;132:106101. https://doi.org/10.1016/j.soildyn.2020.106101.

[15] Villacreses J, Caicedo B, Caro S, Yépez F. A novel procedure to determine shear dynamic modulus and damping ratio for partially saturated compacted fine-grained soils. Soil Dynam Earthq Eng 2020;131:106029. https://doi.org/10.1016/j.soildyn.2019.106029.

[16] Patiño H, Molina-Gómez F, Galindo R, Viana da Fonseca A. Integrated evaluation of stiffness degradation by combining resonant-column, cyclic triaxial and cyclic simple shear tests: application to Riotinto mine tailings. Geomech Energy Environ 2025;41:100652. https://doi.org/10.1016/j.gete.2025.100652.

[17] Sun P, Wang D. Comparison of damping parameters based on the half-power bandwidth methods of viscous and hysteretic damping models. J Vib Control 2023;29(3–4). https://doi.org/10.1177/10775463211054646.

[18] Menard KP, Menard N. Dynamic mechanical analysis. Boca Raton: CRC Press; 2020. https://doi.org/10.1201/9780429190308.

[19] Mezger T. The Rheology Handbook: For Users of Rotational and Oscillatory Rheometers. European Coatings; 2020.

[20] Molina-Gómez F, Viana da Fonseca A. Key geomechanical properties of the historically liquefiable TP-Lisbon sand. Soils Found 2021;61(3):836–56. https://doi.org/10.1016/j.sandf.2021.03.004.

[21] Instruments TA. Rheometer: rheometric series operator's manual. New Castle, DE, USA: TA Instruments; 2006.

[22] Gourves R. Application of the schneebli model in the study of micromechanics of granular media. Mech. Mater. 1993;16(1-2):125–31.

[23] Gourvès R, Mezghani F. Micromécanique des Milieux Granulaires, Approche Expérimentale Utilisant le Modèle de Schneebeli. Rev Fr Geotech 1988;(42):23–34. https://doi.org/10.1051/geotech/1988042023.

[24] Caicedo B. Geotechnics of roads: fundamentals. Boca Raton: CRC Press; 2018. https://doi.org/10.1201/9780429025914.

[25] Molina-Gómez FA. The TP-Lisbon Sand in Partially Saturated Conditions: Experimental Evidence and Physical Modelling Validation. Porto, Portugal: Faculdade de Engenharia, Universidade do Porto; 2023.

[26] Asuero AG, Sayago A, González AG. The correlation coefficient: an overview. Crit Rev Anal Chem 2006;36(1):41–59. https://doi.org/10.1080/10408340500526766.

[27] Phoon K, Ching J. Characterization of geotechnical variability – a multivariate perspective. In: Computer methods and recent advances in geomechanics, Kyoto, Japan; 2014. https://doi.org/10.1201/b17435-10.

[28] Santos JA, Gomes Correia A. Reference Threshold Shear Strain of Soil. Its Application to Obtain an Unique Strain-Dependent Shear Modulus Curve for Soil. In: Proceedings of the 15th International Conference on Soil Mechanics and Geotechnical Engineering. London: International Society for Soil Mechanics and Geotechnical Engineering; 2001. p. 267–70.

[29] Oztoprak S, Bolton MD. Stiffness of sands through a laboratory test database. Geotechnique 2013;63(1):54–70. https://doi.org/10.1680/geot.10.P.078.

[30] De Myttenaere A, Golden B, Le Grand B, Rossi F. Mean absolute percentage error for regression models. Neurocomputing 2016;192:38–48. https://doi.org/10.1016/j.neucom.2015.12.114.

[31] Senetakis K, Anastasiadis A, Pitilakis K. A comparison of material damping measurements in resonant column using the steady-state and free-vibration decay methods. Soil Dynam Earthq Eng 2015;74:10–3. https://doi.org/10.1016/j.soildyn.2015.03.009.

[32] Mog K, Anbazhagan P. Evaluation of the damping ratio of soils in a resonant column using different methods. Soils Found 2022;62:101091. https://doi.org/10.1016/j.sandf.2021.101091.

[33] Patiño H, Molina-Gómez F, Galindo-Aires R. Evaluating the damping ratio of tailings by different experimental methods: case study of riotinto mines. Geosciences 2026;16:173. https://doi.org/10.3390/geosciences16050173.

[34] Roesler SK. Anisotropic shear modulus due to stress anisotropy. J Geotech Eng Div 1979;105(7):871–80. https://doi.org/10.1061/AJGEB6.0000835.

[35] Hardin BO, Blandford GE. Elasticity of particulate materials. J Geotech Eng 1989;115(6):788–805. https://doi.org/10.1061/(ASCE)0733-9410(1989)115:6(788).

[36] Payan M, Khoshghalb A, Senetakis K, Khalili N. Small-strain stiffness of sand subjected to stress anisotropy. Soil Dynam Earthq Eng 2016;88:143–51. https://doi.org/10.1016/j.soildyn.2016.06.004.

[37] Payan M, Jamshidi Chenari R. Small strain shear modulus of anisotropically loaded sands. Soil Dynam Earthq Eng 2019;125:105726. https://doi.org/10.1016/j.soildyn.2019.105726.

[38] Prashant A, Bhattacharya D, Gundlapalli S. Stress-state dependency of small-strain shear modulus in silty sand and sandy silt of ganga. Geotechnique 2019;69(1):42–56. https://doi.org/10.1680/jgeot.17.P.100.